Veterinary Microbiology 236 (2019) 108396

Contents lists available at ScienceDirect

Veterinary Microbiology

journal homepage: www.elsevier.com/locate/vetmic

Mitophagy mediated by BNIP3 and BNIP3L/NIX in urothelial cells of the urinary bladder of cattle harbouring bovine papillomavirus infection

Sante Roperto[a,*], Francesca De Falco[a], Antonella Perillo[b], Cornel Catoi[c], Franco Roperto[d]

[a] Dipartimento di Medicina Veterinaria e Produzioni Animali, Università di Napoli Federico II, Napoli, Italy
[b] Dipartimento di Medicina Veterinaria, Università degli Studi di Bari Aldo Moro, Valenzano, Italy
[c] University of Agricultural Sciences and Veterinary Medicine, Faculty of Veterinary Medicine, Pathology Department, Cluj-Napoca, Romania
[d] Dipartimento di Biologia, Università di Napoli Federico II, Napoli, Italy

ARTICLE INFO

Keywords:
BPV E5 oncoprotein
BNIP3
BNIP3L/Nix
Mitophagy receptors
Bag3
HIF-1α

ABSTRACT

Autophagy is a powerful tool that host cells use to defend against viral infection. Mitophagy, the selective autophagic removal of dysfunctional mitochondria was upregulated in urothelial cancer cells harbouring bovine papillomavirus (BPV) infection, as detected by the expression of BPV E5 protein, the major oncoprotein of bovine Deltapapillomavirus genus. HIF-1α-induced mitophagy receptors, BNIP3 and BNIP3L/Nix, were found to be overexpressed in these cells. The BNIP3 and BNIP3L/Nix receptors were amplified, and amplicon sequencing showed homology between bovine BNPI3 and BNIP3L/Nix sequences deposited in GenBank (accession number: NM_001076366.1 and NM_001034614.2, respectively). The transcripts and protein levels of BNIP3 and BNIP3L/Nix were significantly overexpressed in hypoxic neoplastic cells relative to healthy, non-neoplastic cells. BNIP3 and BNIP3L/Nix interacted with the LC3 protein, a marker of autophagosome (mitophagosome) membrane, ERAS, a small GTPase, and p62, known to be a specific autophagy receptor protein, that plays a role in mitochondrial priming for mitophagy and subsequent elimination. ERAS also interacted with the BPV E5 oncoprotein at mitochondrial level. Furthermore, in anti-Bag3 mitochondrial immunoprecipitates, a complex composed of the Hsc70/Hsp70 chaperone, CHIP co-chaperone, Synpo2, ERAS, LC3, p62, BNPI3, and BNIP3L/Nix was also detected. Bag3 may play a role in mitophagosome formation together with the Synpo2 protein and may be involved in the degradation of Hsc70/Hsp70-bound CHIP-ubiquitinated cargo, in association with its chaperone. ERAS may be involved in mitophagosome maturation via the PI3K signalling pathway. Ultrastructural findings revealed the presence of mitochondria exhibiting severe fragmentation and loss of cristae, as well as numerous mitochondria-containing autophagosomes.

1. Introduction

The maintenance of a healthy and functional mitochondrial network is critical during development as well as throughout life in response to physiological adaptations and stress conditions (Pickles et al., 2018). In order to maintain an intact mitochondrial network, cells have developed quality control systems that allow the removal of damaged or unwanted mitochondria by selective mitochondrial autophagy, called mitophagy, a form of evolutionarily conserved macroautophagy. Mitophagy has been speculated to perform a housekeeping role under steady-state conditions, and is responsible for the timely turnover of aged organelles. Furthermore, to avoid the potential risks associated with dysfunctional mitochondria, mitophagy can be enhanced to selectively remove damaged mitochondria. Multiple mitophagy pathways operate within the cell. Currently, the mechanisms of mitophagy can be classified in two groups, i.e. Parkin-dependent and Parkin-independent mitophagy (Youle and Narendra, 2011), the latter being mediated by mitophagy receptors, which are proteins that are localised to the outer mitochondrial membrane (OMM).

Different types of mitophagy receptors have been identified in mammalian cells such as BNIP3 (Bcl-2/adenovirus E1B 19-kDa-interacting protein 3) and BNIP3-like (BNIP3L, also known as NIX) as well as FUNDC1 (FUN14 domain containing protein 1) (Liu et al., 2014). Furthermore, a new mitophagy receptor, known as FKBP8, has been identified to mediate Parkin-independent mitophagy (Bhujabal et al., 2017). Recently, a mitophagy receptor was identified in the inner mitochondrial membrane (IMM) and named prohibitin 2 (PHB2) (Wei et al., 2017). It plays a crucial role in both Parkin-dependent and Parkin-independent mitophagy (Wei et al., 2017). One common feature of mitophagy receptors is that they harbour an LC3-interacting region

* Corresponding author.
E-mail address: sante.roperto@unina.it (S. Roperto).

https://doi.org/10.1016/j.vetmic.2019.108396
Received 25 May 2019; Received in revised form 20 August 2019; Accepted 20 August 2019

(LIR) that interacts with LC3, thus promoting the sequestration of mitochondria into the isolation membrane or phagophore (Wei et al., 2015; Bhujabal et al., 2017; Wei et al., 2017).

BNIP3 and BNIP3L/Nix are multifunctional mitochondrial outer membrane proteins that are related to the BH3-only family (Wei et al., 2015). Both mitophagy receptors are known to mediate mitophagy during hypoxia, which, in turn, is responsible for their upregulation (Zhang and Ney, 2009; Liu et al., 2014). Although BNIP3 and NIX are primarily under transcriptional control, their mitophagic activity is also activated by post-translational modification. Indeed, it has been shown that phosphorylation of serine at positions 17 and 24 adjacent to the LIR of BNIP3 as well as serine at positions 34 and 35 in the LIR domain of NIX strengthens the interaction of these receptors with LC3B to enhance mitophagy (Rogov et al., 2017)

BNIP3 was recently shown to play an important role in regulating cell proliferation via MAPK activation. Furthermore, NIX, which plays a critical role in the maturation and differentiation of erythroid cells, is required for mitochondrial network remodelling during cardiac progenitor cell differentiation (Lampert et al., 2019). It is believed that both BNIP3 and BNIP3L/Nix play a role in the progression of cancer and metastasis (Chourasia and Macleod, 2015). Indeed, it is believed that BNIP3-mediated mitophagy delays the progression to metastatic disease. It is accepted that mitophagy, in general, is a tumour suppression mechanism (Chourasia et al., 2015; Bernardini et al., 2017). In particular, impairment of mitophagy mediated by FUNDC1 was found to correlate negatively with the prognosis of cervical cancer caused by high-risk HPVs (Hou et al., 2017). Furthermore, it has been shown that HPV early protein 7 (E7) enhances ceramide-mediated mitophagy, thus, inducing tumour suppression (Thomas et al., 2017). Indeed, several studies have revealed that deregulated expression of mitophagy receptors can promote cancer proliferation and migration. In this context, it has been suggested that an improved selective autophagy during viral infections correlates negatively with tumour development, whereas impairment of the autophagy and mitophagy machinery promotes progression to metastasis in many virus malignancies, including the malignancies associated with HPVs (Mattoscio et al., 2018).

Bovine papillomaviruses (BPVs) comprise 28 types classified into five genera (https://pave.niaid.nih.gov/; Crespo et al., 2019). The Deltapapillomavirus (*δ*PV) genus is composed of four high-risk members, namely BPV-1, BPV-2, BPV-13, and BPV-14 (Daudt et al., 2018). Although all members of the bovine *δ*PVs play an important etiological role in both cutaneous and bladder tumours, BPV-2 and BPV-13 are the most important infectious agents associated with urothelial tumours, being found very commonly in some breeds of pasture-residing cattle that graze on bracken fern-infested lands (Campo et al., 1992; Roperto et al., 2013, 2016).

The transforming activity of the *δ*PVs, even in the absence of other viral genes, is mainly driven by the E5 protein, the major oncoprotein of *δ*PVs, (DiMaio and Petti, 2013), via multiple molecular pathways, including the embryonic stem (ES) cell-expressed Ras (ERas) pathway (Russo et al., 2016).

The aim of the present paper was to report a mechanistic study about molecular and ultrastructural findings that characterize the BNIP3- and BNIP3L/Nix-mediated mitophagy in bovine PV-infected urothelial cells.

2. Materials and methods

2.1. Ethics statement

In this study, we did not perform any animal experiments. All the samples were collected post-mortem from slaughterhouses, and therefore, no ethicals approval was required.

2.2. Tumour samples

Neoplastic bladder mucosa samples from 19 cows suffering from clinical chronic enzootic haematuria were collected from public slaughterhouses after bladder neoplasms had been identified during routine meat inspection. Bladder mucosa samples from 15 apparently healthy cows were also collected. All bladder mucosa samples were subdivided and either fixed in 10% buffered formalin for microscopic investigation or immediately frozen in liquid nitrogen and stored at −80 °C for subsequent molecular biology analysis. Furthermore, they were fixed in 4% glutaraldehyde in 0.1 M phosphate buffer (pH 7.4) for ultrastructural investigation.

2.3. Histopathology

The tissues were processed routinely for paraffin embedding. Histological diagnosis was carried out using 5-μm-thick haematoxylin-eosin (HE)–stained sections based on previously suggested morphological criteria (Roperto et al., 2010).

2.4. Transmission electron microscopy (TEM)

All bladder samples were fixed in 4% glutaraldehyde in 0.1 M phosphate buffer (pH 7.4) for 2–3 h. They were then post-fixed with 1% osmium tetroxide (OsO_4) in the same buffer for 1 h and washed again in 0.1 M phosphate buffer (pH 7.4); then, they were dehydrated using treatments with serially-graded alcohol, following which, they were embedded in Agar Low Viscosity Resin (AGR 1078) (Agar Scientific Limited, Essex, England). Semi-thin sections (400 nm) were cut with a glass knife on an EM UC6 ultramicrotome (Leica Microsystems) and stained with 1% toluidine blue. Ultra-thin sections (60–70 nm) were obtained using the same ultramicrotome with a diamond knife and collected onto 300-mesh copper grids coated with formvar. Counterstaining was performed with lead citrate and uranyl acetate. The sections were observed using a JEOL JEM-1011 transmission electron microscope (JEOL, Tokyo, Japan) equipped with a thermionic tungsten filament at an acceleration voltage of 100 kV. Images were taken using a Morada cooled slow-scan CCD camera (3783 × 2672 pixels) and micrographs were taken with iTEM software (Olympus Soft Imaging System GmbH, Munster, Germany).

2.5. Antibodies

Mouse and rabbit antibodies against BNIP3 and BNIP3L/Nix were obtained from Santa Cruz Biotechnology (TX, USA) (sc-56167) and Cell Signaling (LID, NL) (12,396), respectively. Rabbit antibodies against Eras and Synpo2 were obtained from Biorbyt (CA, USA), rabbit antibodies against LC3 and HIF-1α were purchased from Novus Biologicals (CO, USA); rabbit antibody against Bag3 was obtained from Biouniversa (AV, IT); and mouse antibodies against p62, Hsc70/Hsp70, CHIP, and β-actin were obtained from Santa Cruz Biotechnology (TX, USA). Rabbit polyclonal antiserum against E5 (recognizing the C-terminal 14 amino acids of the BPV E5 protein) was kindly provided by Prof. DiMaio, Yale University, New Haven, USA.

2.6. RNA extraction and reverse transcription (RT)-PCR

Total RNA was extracted from all neoplastic and non-neoplastic bladder mucosa samples using an RNeasy Mini Kit (Qiagen TM, ME, DE), in accordance with the manufacturer's instructions. Genomic DNA was removed from the RNA preparations using RNase-free DNase I from Fermentas Life Sciences (Thermo Fisher Scientific, MA, USA). One microgram of the total RNA was used to generate a single strand of cDNA using the QuantiTect Reverse Transcription Kit (Qiagen TM, ME, DE), according to the manufacturer's instructions. PCR was performed with a specific primer set designed by the Primer3 online tool for the E5 gene

of BPV-2, BPV-13, BNIP3 and BNIP3L/Nix. The following primers were used: BPV-2 E5 ORF forward 5′-CACTGCCATTTGTTTTTTTC-3′, reverse 5′-GGAGCACTCAAAATGATCCC-3′; BPV-13 E5 ORF forward 5′-CACTG CCATTTGGTGTTCTT-3′, reverse 5′- AGCAGTCAAAATGATCCCAA-3′; BNIP3 forward 5′-GAAGAACAGCTCCCAGTCCG-3′, reverse 5′−CCGA CTGGACCAATCCCAAA-3′ and BNIP3L/Nix forward 5′-ACTTAGTAGA ACAGCCGCCG-3′, reverse 5′−CCACCCAGGAACTGTTGAGG-3′. Conditions used for PCR were: 94 °C for 5 min, followed by40 cycles of 95 °C for 30 s, 58 °C for 30 s and 72 °C for 30 s.

2.7. Sequence analysis

PCR products, obtained by RT-PCR, were purified by Qiaquick PCR purification Kit (Qiagen TM, ME, DE) and bi-directionally sequenced using a BigDye_Terminator v1.1 Cycle Sequencing Kit (Applied Biosystems, CA, USA), following the manufacturer's recommendations. The sequences were dye-terminator removed by DyeEx 2.0 spin kit (Qiagen TM, ME, DE) and run on a 3500 Genetic Analyser (Applied Biosystems, CA, USA). Electropherograms were analysed using Sequencing analysis v5.2 and sequence scanner v1.0 software (Applied Biosystems, CA, USA). The sequences obtained were analysed by BLAST.

2.8. Real time RT-PCR

To perform real time RT- PCR analysis, total RNA and cDNA from 19 bovine urinary bladder tumour and 15 normal urothelium samples were generated as reported above. Real time PCR was carried out on a Bio Rad CFX Connect™ Real Time PCR Detection System (Bio Rad Hercules, CA, USA) using iTAq Universal SYBR® Green Supermix (Bio Rad Hercules, CA, USA). Each reaction was set in triplicate and the primers used for BNIP3 and BNIP3/Nix were the same as those used for RT-PCR. The PCR conditions used were: 95 °C for 10 min, followed by 40 cycles of 94 °C for 15 s, 56 °C for 30 s, followed by a melting curve. The relative quantification (RQ) was carried out using CFX Manager™ software, based on the equation $RQ = 2^{-\Delta\Delta Cq}$, where Cq is the quantification cycle to detect fluorescence. Cq data were normalised to the reference β-actin gene (forward: 5′- TAGCACAGGCCTCTCGCCTT CGT-3′, reverse 5′-GCACATGCCGGAGCCGTTGT-3′).

2.9. Statistical analysis

Results are presented as means ± SE. The expression levels were assessed by one-way ANOVA, followed by Tukey's test for multiple comparisons of means, using GraphPad PRISM software version 8 (GraphPad Software, San Diego, CA). P values ≤ 0.05 were considered statistically significant.

2.10. Western blot analysis

Healthy and neoplastic bovine urothelial samples were lysed in RIPA buffer (50 mM Tris−HCl (pH 7.5), 1% Triton X-100, 400 mM NaCl, 1 mM EDTA, 2 mM PMSF, 1.7 mg/mL Aprotinin, 50 mM NaF, and 1 mM sodium orthovanadate). The protein concentration was measured using the Bradford assay (Bio-Rad, CA, USA). For western blotting, 50 µg of lysate proteins were heated to 90 °C in 4X premixed Laemmli sample buffer (Bio-Rad, CA, USA). They were centrifuged, subjected to SDS-PAGE, and transferred onto nitrocellulose membranes (GE Healthcare, UK, RPN303D). The membranes were blocked with TBST (TBS and 0.1% Tween 20) containing 5% no-fat dry milk for 1 h at room temperature, and subsequently incubated overnight at 4 °C with primary antibodies before being listed. The membranes were then washed thrice with TBST, incubated for 1 h at room temperature with goat anti-rabbit (Bio-Rad, CA, USA) and goat anti-mouse (Bio-Rad, CA, USA) HRP-conjugated secondary antibodies diluted at 1:2000 in TBST, and washed thrice with TBST. Immunoreactive bands were detected using Western Blotting Luminol Reagent (Santa Cruz Biotechnology, TX, USA) and ChemiDoc XRS Plus (Bio-Rad, CA, USA). Images were acquired using Image Lab Software version 2.0.1.

2.11. Cell fractionation and mitochondria isolation

Mitochondria from nine bovine urothelial tumour samples and six bladder samples from healthy cows were prepared using the Qproteome mitochondria isolation kit (Qiagen TM, ME, DE). Briefly, 60 mg slices were cut from each tissue, washed in 0.9% NaCl, and incubated for 10 min at 4 °C in lysis buffer. The homogenate was centrifuged at 1000 xg for 10 min at 4 °C, and the supernatant was designated as the cytosolic fraction. The pellet was resuspended in disruption buffer and passed through a 26-gauge needle 15 times. Enriched nuclei fraction was pelleted by centrifugation at 1000 xg for 10 min and homogenised in a disruption buffer. To obtain the enriched mitochondrial fraction, the supernatant was centrifuged at 6000 xg for 10 min at 4 °C. The pellet contained the mitochondria and the supernatant constituted the microsomal fraction. The pellet was resuspended in mitochondria storage buffer. All buffers, except mitochondria storage buffer, were supplemented with protease inhibitors at 1:100 ratio, provided within the kit. Protein concentration in the different fractions was determined with Bio-Rad protein assay (Bio-Rad, CA, USA).

2.12. Mitochondria immunoprecipitation

Mitochondrial extracts from normal and pathological bladders, obtained as previously described, were immunoprecipitated. Protein samples (100 µg) were incubated with anti-BNIP3, anti-BNIP3L/Nix, anti-BAG-3, anti-ERAS primary antibodies for 1 h at 4 °C with gentle shaking. Following the incubation, centrifugation (1000 xg for 5 min at 4 °C) was carried out, and the samples were collected and incubated overnight with 30 µL of Protein A/G-Plus Agarose (sc-2003) (Santa Cruz Biotechnology, TX, USA) at 4 °C. Immunoprecipitates were washed four times in complete lysis buffer (as described above), and separated on polyacrylamide gels. Following the transfer of proteins, membranes were blocked for 1 h at room temperature in 5% bovine serum albumin, and incubated overnight with respective primary antibodies at 4 °C. After three washes in tris-buffered saline, membranes were incubated with the respective secondary antibodies for 1 h at room temperature. Chemiluminescent signals were then developed using Western Blotting Luminol Reagent (Santa Cruz Biotechnology, TX, USA), and detected by the ChemiDoc XRS Plus gel documentation system (Bio-Rad, CA, USA).

3. Results

3.1. Ultrastructural findings

Mitochondrial ultrastructural abnormalities resulting in fragmentation and loss of cristae leading to a moderate electron-dense matrix were peculiar features of urothelial cancer cells. Furthermore, the ultrastructural pattern was also characterized by the presence of phagophores, mitophagosomes, and mitolysosomes, which revealed that the dysfunctional mitochondria could be eliminated by mitophagy in these cells (Fig. 1).

As hypoxia, a common condition of cancer cells, is an important cause for extensive fragmentation of mitochondria as well as loss of cristae and both of them lead to mitophagy (Liu et al., 2014), we wanted to investigate whether urothelial cancer cells infected by BPVs, under hypoxic conditions, could act like tumour cells infected by human papillomaviruses (HPVs) (Guo et al., 2014). Therefore, we studied the expression of hypoxia-inducible factor 1α (HIF-1α), an oxygen-sensitive subunit, which is known to be induced by hypoxia. Western blot analysis revealed a statistically significant overexpression of HIF-1α in neoplastic bladder mucosa in comparison with non-neoplastic bladder samples, which showed that urothelial cells infected by BPVs

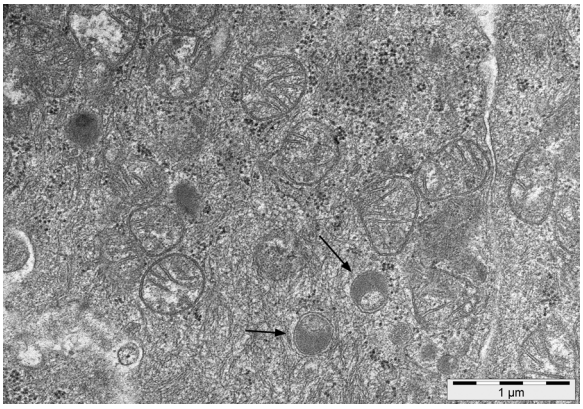

Fig. 1. Ultrastructural pattern of urothelial cancer cells infected by BPVs showing mitochondrial abnormalities (fragmentation and loss of cristae), and several mitolysosomes (arrows).

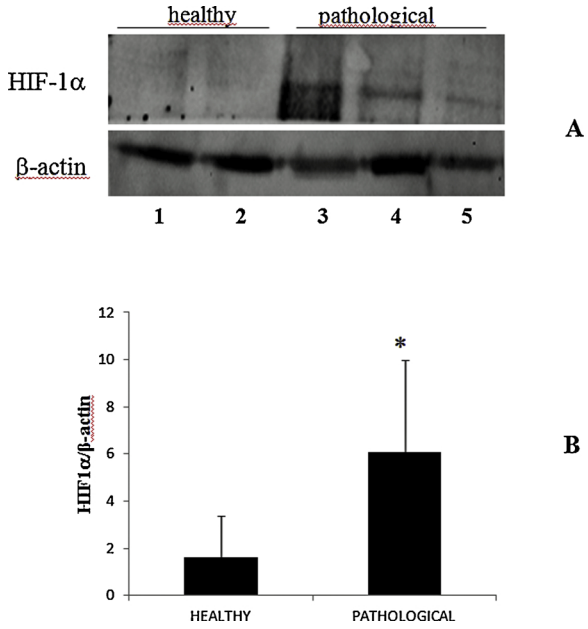

Fig. 2. Western blot analysis HIF-1α for healthy and neoplastic bladder mucosa samples infected by BPVs. Lanes 1–2: bladder mucosa samples from healthy cows; Lanes 3–5: three representative papillary urothelial cancers. The lower part of the western blot showed a densitometric analysis. Statistically significant overexpression of HIF-1α protein levels was indicated in neoplastic bladder mucosa samples (* $p < 0.05$).

were actually under hypoxic conditions as this factor is known to be highly expressed in hypoxic microenvironment (Daskalaki et al., 2018) (Fig. 2).

3.2. Expression of mitophagy receptors: BNIP3 and BNIP3L/NIX

Hypoxia is known to induce selective autophagy of mitochondria by mitophagy receptors (Liu et al., 2014). Moreover, HIF-1α appears to be involved in the regulation of expressions of BNIP3 and BNIP3L/Nix (Zhang and Ney, 2009; Chourasia and Macleod, 2015; Daskalaki et al., 2018). Firstly, we wanted to investigate if BNIP3 and BNIP3L/Nix were constitutively expressed in urothelial cells of the urinary bladder of cattle. Therefore, we performed RT-PCR analysis on cDNA obtained from non-neoplastic and neoplastic bladder samples, detecting both 103 and 102 bp transcript sequences, the alignment of which showed a 100% identity with bovine BNIP3 and BNIP3L/Nix sequences deposited in GenBank (accession number: NM_001076366.1 and NM_001034614.2, respectively) (Fig. 3). Real time RT-PCR showed a significant increase both of BNIP3 and BNIP3L/Nix in six and three neoplastic bladder samples, respectively (Fig. 4). Western blot analysis on total extracts confirmed a statistically significant overexpression both of BNIP3 and BNIP3L/Nix receptor proteins in neoplastic bladder samples compared to non-neoplastic bladder samples (Fig. 5), which showed that these receptors are transcriptional targets of HIF-1α in cattle. Furthermore, we carried out western blot analysis for subcellular fractions, and BNIP3 and BNIP3L/Nix were found to be overexpressed both in the mitochondrial and cytosolic fractions obtained from neoplastic bladder samples in comparison with mitochondrial and cytosolic fractions obtained from non-neoplastic bladder samples (Fig. 6).

3.3. The network of interactors associated with BNIP3 and BNIP3L/Nix

It is believed that BNIP3 and BNIP3L/Nix can interact, through their LIR, with LC3, an autophagy-related protein, that could be required for phagophore growth and cargo incorporation rather than for phagophore initiation (Ney, 2015), and this interaction is enhanced by hypoxia (Liu et al., 2014; Ney, 2015; Rogov et al., 2017). To explore whether this interaction occurs in naturally occurring papillomavirus infections, we performed western blot analysis on mitochondrial and cytosolic fractions from both neoplastic and non-neoplastic bladder mucosa samples immunoprecipitated by anti-BNIP3 and anti-BNIP3L/Nix antibodies, and we detected the presence of LC3 protein, which demonstrated that BNIP3 and BNIP3L/Nix are physically associated with LC3 protein. This mechanistic interaction was more evident in neoplastic than in non-neoplastic bladder mucosa samples, indicating the build-up of an accentuated autophagosome (mitophagosome) formation in urothelial cancer cells under hypoxia. Furthermore, p62, an autophagy receptor protein, can interact with LC3 thus recruiting autophagosomal membranes leading to the formation of mitophagosome and play a role in priming the damaged mitochondria for recognition, and thus, promoting their subsequent sequestration into mitophagosomes (Wei et al., 2015). Western blot analysis, performed on BNIP3 as well as BNIP3L/Nix immunoprecipitates, detected the presence of p62 protein in mitochondrial and cytosolic fractions. Therefore, a complex composed of BNIP3, BNIP3L/Nix, LC3 and p62 was detected at the mitochondrial level (Fig. 7).

Taken together, molecular and ultrastructural findings of our study provided the evidence that mitophagy mediated by both BNIP3 and BNIP3L/Nix is activated in urothelial cancer cells infected by BPVs.

3.4. ERAS interacts with the BPV E5 oncoprotein and BNIP3- and BNIP3L/Nix

It has been shown that the small GTPase Rheb (Ras homolog enriched in brain) can be recruited to the mitochondrial membrane, which promotes mitophagy through a physical interaction with mitophagy receptors and the autophagosomal protein, LC3 (Melser et al., 2013).

Unlike humans, Eras is expressed in bovine cells of adult animals and forms a constitutive complex along with PDGFβR resulting in activation of Akt signalling pathway (Roperto et al., 2017). Because of their atypical carboxyl-terminal sequences, ERAS shares several common functions with Rheb, such as the activation of the phosphatidylinositol 3-kinase (PI3K) signalling pathway (Takahashi et al., 2005). PI3K produces phosphatidylinositol 3-phosphate that plays a role in autophagosome (mitophagosome) formation.

To investigate whether ERAS plays a role in mitophagy, we obtained mitochondrial and cytosolic immunoprecipitates from neoplastic and non-neoplastic bladder mucosa samples using an anti-ERAS antibody. Western blot analysis unveiled the presence both of BNIP3- and BNIP3L/Nix as well as LC3, which showed that ERAS interacted with both the mitophagy receptors and LC3. Therefore, a complex composed of ERAS/BNIP3/BNIP3L/Nix/LC3 was seen at mitochondrial and cytosolic levels. Each

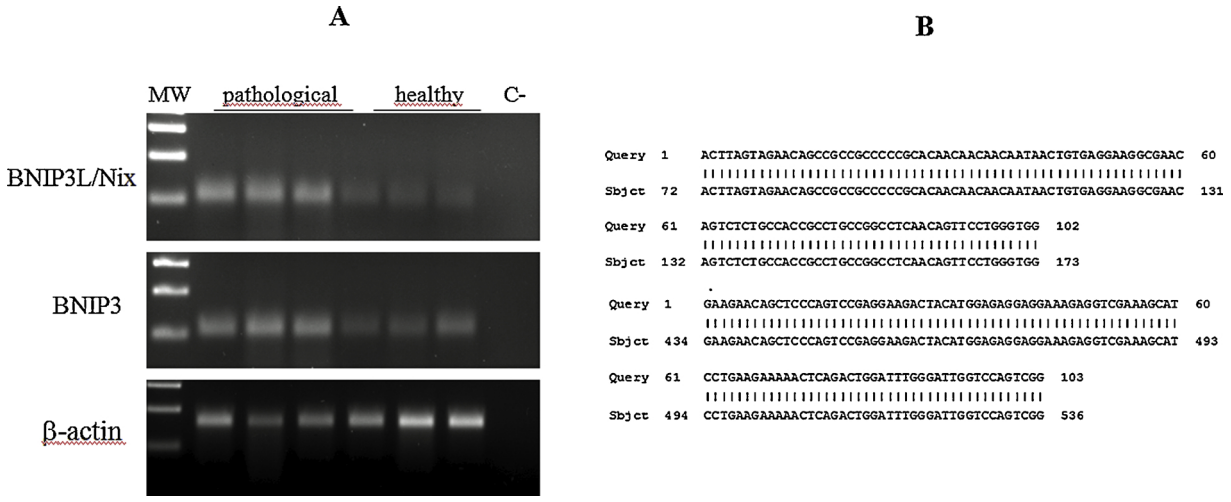

Fig. 3. RT-PCR analysis of BNIP3 and BNIP3/Nix mRNA expression in healthy and neoplastic bovine bladders. (A) MW: molecular weight marker (100 bp ladder); lanes 1-3: healthy mucosa samples; lanes 4 - 6: three representative urothelial endoluminal cancers; lane C-: negative control. (B) Alignment of the sequences shows 100% identity with: *Bos taurus* BCL2 interacting protein 3 (BNIP3) mRNA (accession number: NM_001076366.1) and *Bos taurus* BCL2 interacting protein 3 like (BNIP3L) mRNA (accession number: NM_001034614.2).

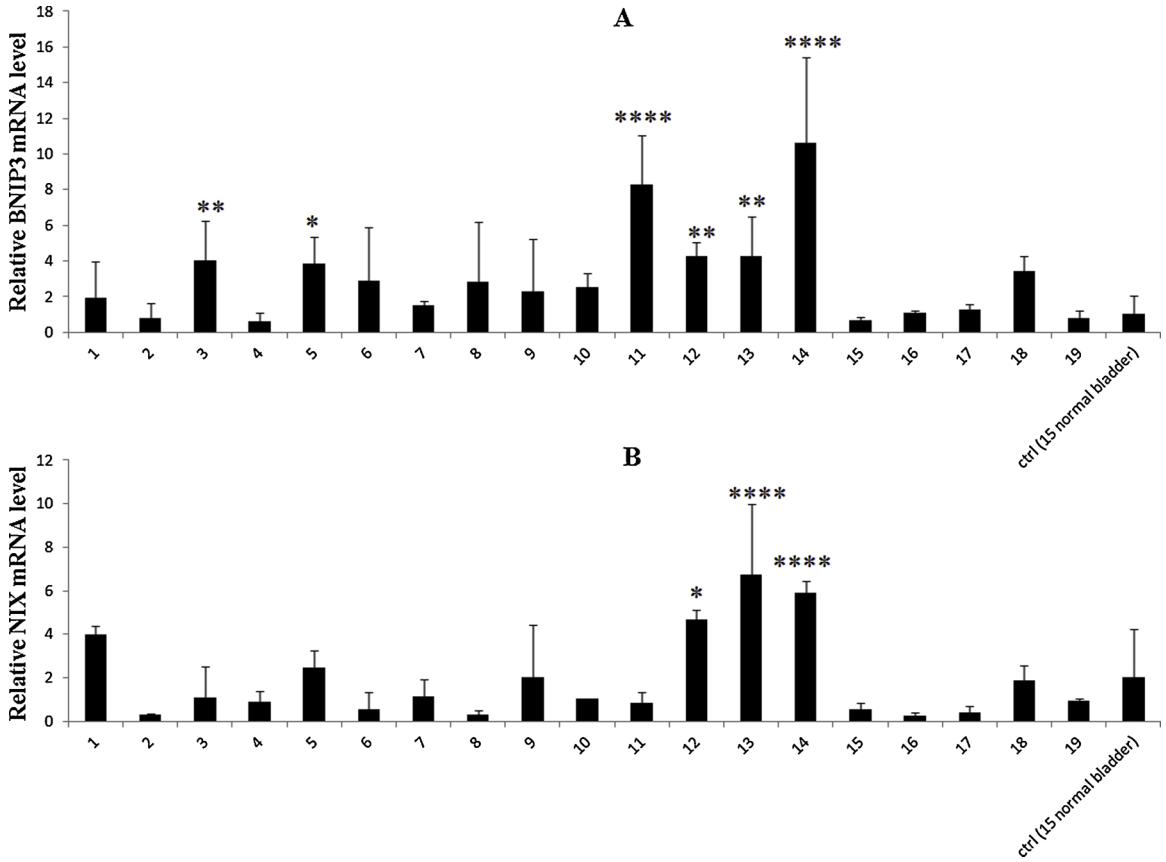

Fig. 4. (A) Real time RT-PCR. BNIP3 mRNA levels in 15 normal controls (CTRL) and in 19 neoplastic bladder samples. In particular, it was shown that, in 3, 5, 11, 12, 13, and 14 bladder samples there was a statistically significant difference in expression of BNIP3 mRNA compared to normal bladders (* $p \leq 0.05$). Data is expressed as mean ± S.E.M. of three separate experiments performed in triplicates * $p < 0.05$; ** $p < 0.01$; **** $p < 0.0001$. (B) Real time RT-PCR. BNIP3L/Nix mRNA levels in 15 normal controls (CTRL) and in 19 neoplastic bladder samples. In particular, it was shown that, in 12, 13, and 14 bladder samples there was a statistically significant difference in expression of BNIP3L/Nix mRNA compared to normal bladders (* $p \leq 0.05$). Data is expressed as mean ± S.E.M. of three separate experiments performed in triplicates ** $p < 0.01$; **** $p < 0.0001$.

component of this complex appeared to be overexpressed in neoplastic bladder samples compared with non-neoplastic bladder samples. Furthermore, it has previously been shown that ERAS plays a crucial role in BPV infection (Russo et al., 2016). Then, we studied whether BPV E5 oncoprotein, normally localised as a dimer to the membranes of the endoplasmic reticulum and Golgi apparatus (Schlegel et al., 1986), could be translocated at the mitochondrial level. Therefore, we performed western blot analysis for BPV E5 and detected its expression on anti-ERAS immunoprecipitates, which suggested that the BPV E5 oncoprotein translocated to the mitochondrial membrane (Fig. 8).

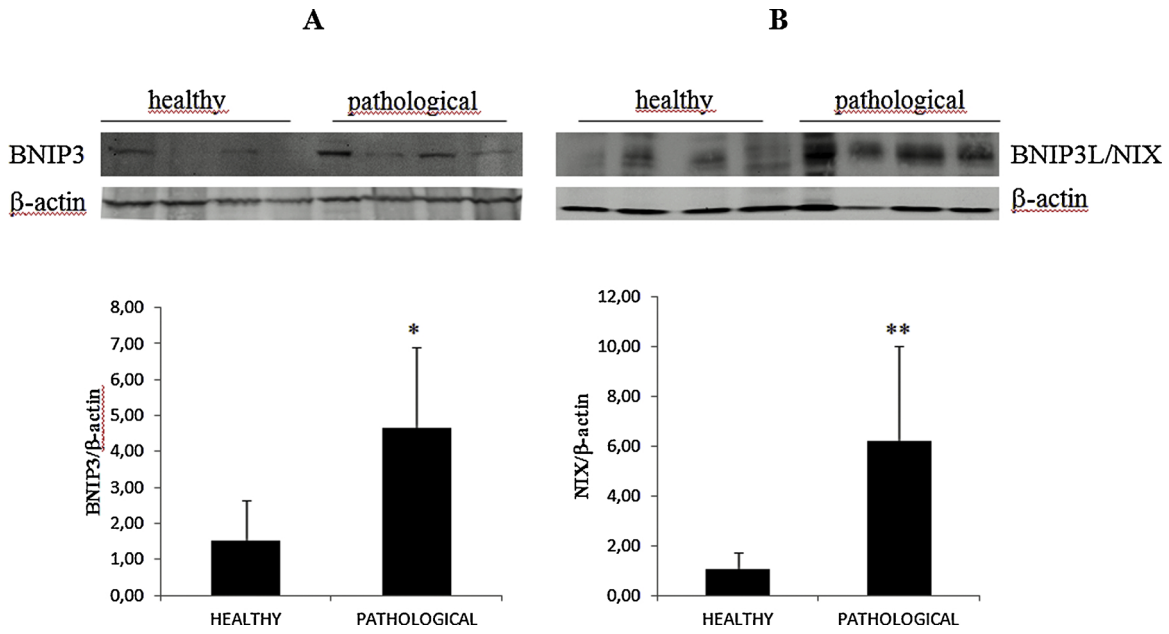

Fig. 5. BNIP3 and BNIP3L/Nix western blot analysis on healthy and neoplastic bladder mucosa samples. Densitometric analysis detected statistically significant overexpression of BNIP3 and BNIP3L/Nix protein levels in the neoplastic bladder mucosa samples (* $p < 0.05$, **$p < 0.01$).

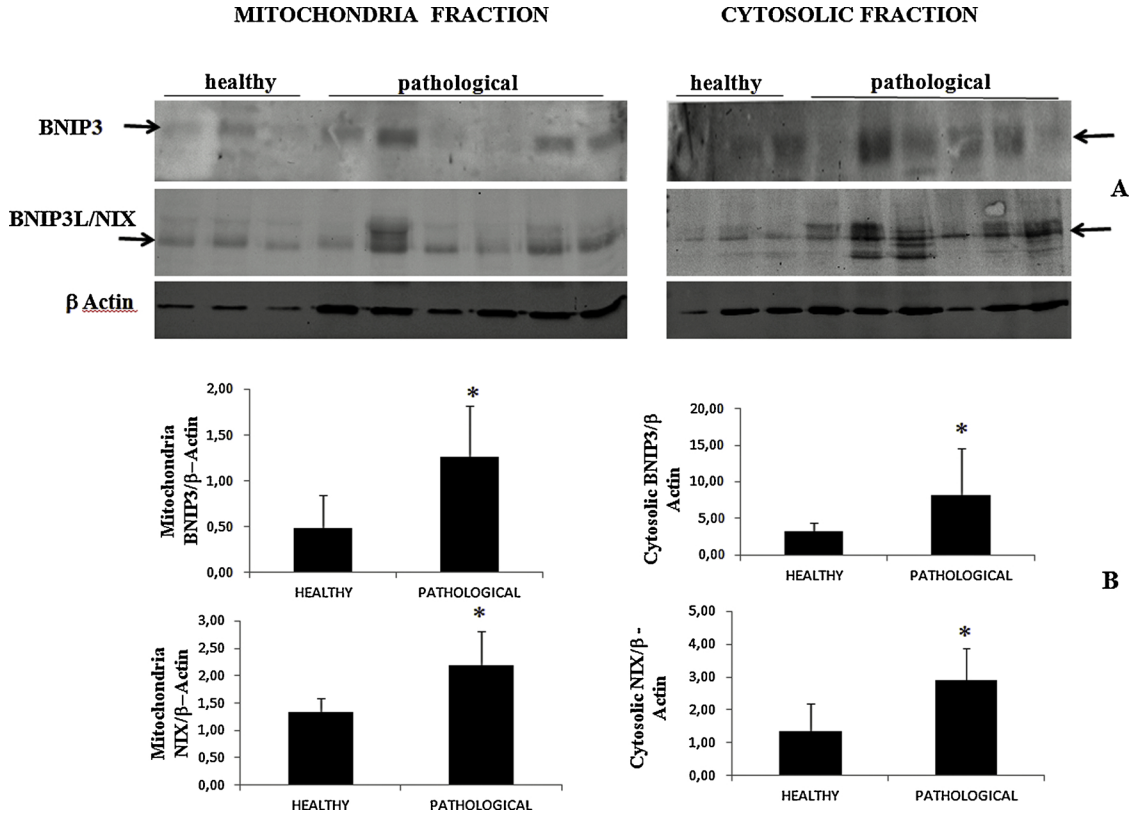

Fig. 6. Western blot analysis of BNIP3 and BNIP3L/Nix in mitochondrial and cytosolic subcellular fractions. Ten micrograms of different subcellular protein fractions from healthy and neoplastic mucosa samples were electrophoresed through a denaturing polyacrylamide gel, electroblotted and hybridised with anti-BNIP3, anti-BNIP3L/Nix, or anti-β-actin antibody (as a loading control). Densitometric analysis of BNIP3 and BNIP3L/Nix mitochondrial and cytosolic proteins was performed in comparison with β-actin protein levels. The calculations were based on three independent determinations. The values for the latter are expressed as a percentage of the average values for the healthy samples (*$p < 0.05$).

3.5. Protein network of interactors mediated by Bag3 at the mitochondrial level

It has been suggested that the Bag3-containing chaperone/co-chaperone complex recognizes ubiquitinated cargo and transports them to be degraded (Park et al., 2017). Bag3 and Hsc70/Hsp70 play a role in Parkin-dependent and FUNDC1-mediated mitophagy (Tahrir et al., 2017; Roperto et al., 2019a). Emerging evidence supports the mechanistic insights that these cytosolic proteins can be recruited to

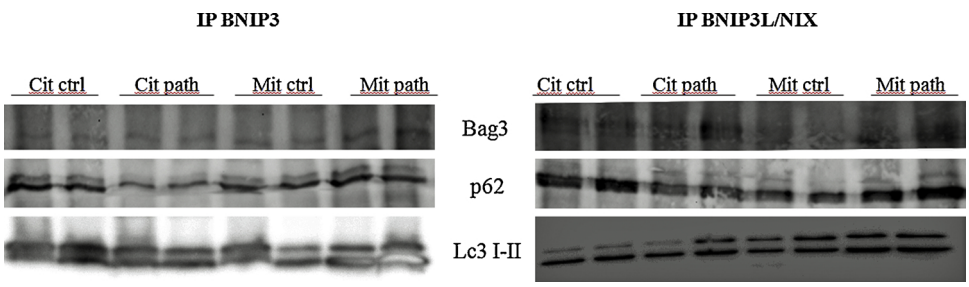

Fig. 7. Mitochondrial and cytosolic immunoprecipitation by anti-BNIP3 and anti-BNIP3L/Nix antibodies in non-neoplastic and neoplastic bladder samples. Western blot analysis revealed the presence of Bag3, LC3, and p62 in both BNIP3 and BNIP3L immunoprecipitates.

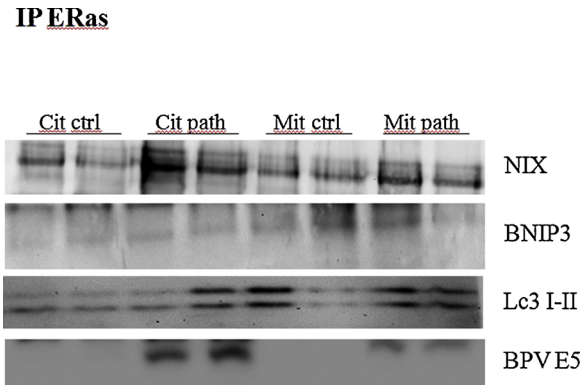

Fig. 8. Mitochondrial and cytosolic immunoprecipitates by an anti-ERAS antibody from neoplastic and non-neoplastic bladder samples. Western blot analysis detected the presence of both BNIP3 and BNIP3L/Nix as well as LC3 and BPV E5.

mitochondria (Tahrir et al., 2017; Roperto et al., 2019a).

We investigated whether Bag3 co-chaperone could be localised at the mitochondrial level and potentially involved in mitophagy mediated by BNIP3 and BNIP3L/Nix. Therefore, we performed western blot analysis, and detected Bag3 expression in all subcellular fractions, including mitochondria (Fig. 9). Furthermore, Bag3 was significantly overexpressed in the mitochondrial subcellular fraction of neoplastic cells compared to non-neoplastic cells (Fig. 9). Next, we carried out immunoprecipitation of mitochondrial subcellular fractions with an anti-Bag3 antibody, and detected, for the first time, through western blot analysis, the presence of both BNIP3 and BNIP3L/Nix, Hpc70/Hsp70, and CHIP, an HSC70-interacting E3 ubiquitin ligase that promotes the ubiquitination and subsequent degradation of HSC70 clients, which indicated the generation of a mitochondrial complex composed of these mitophagy receptors, Hpc70/Hsp70 chaperone as well as Bag3 and CHIP co-chaperones (Fig. 10). It is conceivable that Bag3, in association with Hsc70/Hsp70, may contribute to the transport for degradation of CHIP-ubiquitinated cargo. In addition, western blot analysis unveiled the presence of ERAS, p62, and LC3 within the mitochondrial immunoprecipitates obtained with Bag3 (Fig. 10).

It has been suggested that interactions between Bag3 and synaptopodin 2 (Synpo2), a cytoskeleton adaptor protein that acts as a tumour suppressor in the bladder, play a crucial role in autophagosome formation in mechanically strained cells during general autophagy. To explore whether similar potential cooperation occurred during the mitophagy in bovine bladder mucosa samples, we investigated the mitochondrial immunoprecipitates obtained with anti-Bag3 antibody, and detected the presence, of Synpo2 by western blot (Fig. 10). Taken together, these molecular findings are consistent with the assumption that Bag3 and Synpo2 are both involved in the formation of mitophagosome membrane during mitophagy.

Our mechanistic findings are consistent with the assumption that during spontaneous diseases by papillomavirus infection, there is an interaction of a network of interactors (Synpo2, ERAS, LC3, and p62) mediated by Bag3 for mitophagosome formation. Furthermore, BNIP3- and BNIP3L/Nix may be involved in selective removal of the damaged mitochondria via LC3/p62 pathway as well as of the CHIP-ubiquitinated cargos translocated to mitochondrial membrane by Hsc70/Hsp70, including BPV E5 oncoprotein.

4. Discussion

Our study reports, for the first time, that the mitophagy receptors, BNIP3 and BNIP3L/Nix, are constitutively expressed in urothelial cells of the urinary bladder of cattle. In line with their expression pattern, which is known to be tissue-specific (Springer and Macleod, 2016), being most strongly expressed in mechanically strained cells of skeletal muscle, heart, lung and kidney (Lampert et al., 2019), our insights suggested that the mitophagy receptors play functional role(s) in the urothelial cells at baseline. As it has been suggested that the regulation of mitochondrial mass also occurs routinely under physiological conditions (Chourasia et al., 2015; Moyzis and Gustafsson, 2019), our mechanistic insights suggested that mitophagy receptors may be involved in degradation mechanisms that contributes to mitochondrial turnover of the urothelial cells.

Our current study showed that BPV-2 and BPV-13 E5 transcripts were detected in all neoplastic bladder samples, which confirms that BPV infection is very common in some breeds of cattle that graze on lands rich in bracken fern (Roperto et al., 2019a; Russo et al., 2019). Furthermore, this study reported that both BNIP3 and BNIP3L/Nix were upregulated and overexpressed in BPV-associated urothelial cancer cells which were under hypoxic stress, as shown by the overexpression of HIF-1α, which was very likely promoted by BPV E5 oncoprotein, as already shown for E6 and E7 oncoproteins of HPVs (Nakamura et al., 2009; Rodolico et al., 2011; Guo et al., 2014). The ultrastructural pattern of urothelial cancer cells was characterised by the presence of severe abnormalities of mitochondria, many of which were sequestered in autophagosomes (mitophagosomes). Both BNIP3 and BNIP3L/Nix interacted with LC3, a protein marker for autophagosomes, which is required for specific cargo recognition and incorporation (Ney, 2015; Rogov et al., 2017), and p62, which plays a role in mitochondrial priming for mitophagy machinery and subsequent elimination (Moyzis and Gustafsson, 2019). LC3-p62 complex is known to be a part of a mechanism involved in recruitment of the autophagy machinery to mitochondria (Zhang and Ney, 2011).

Molecular and ultrastructural findings of our study showed that a form of mitophagy activated by hypoxia and mediated by BNIP3 and BNIP3L/Nix occurs in the urothelial cancer cells harbouring BPV infection.

ERAS was detected, for the first time, in BNIP3 and BNIP3L/Nix mitochondrial immunoprecipitates. Furthermore, BPV E5 oncoprotein, BNIP3 and BNIP3L/Nix were found in mitochondrial fractions immunoprecipitated by an anti-ERAS antibody. It is conceivable that ERAS may be recruited to the outer mitochondrial membrane (OMM) to facilitate the interaction between BNIP3 as well as BNIP3L/Nix and

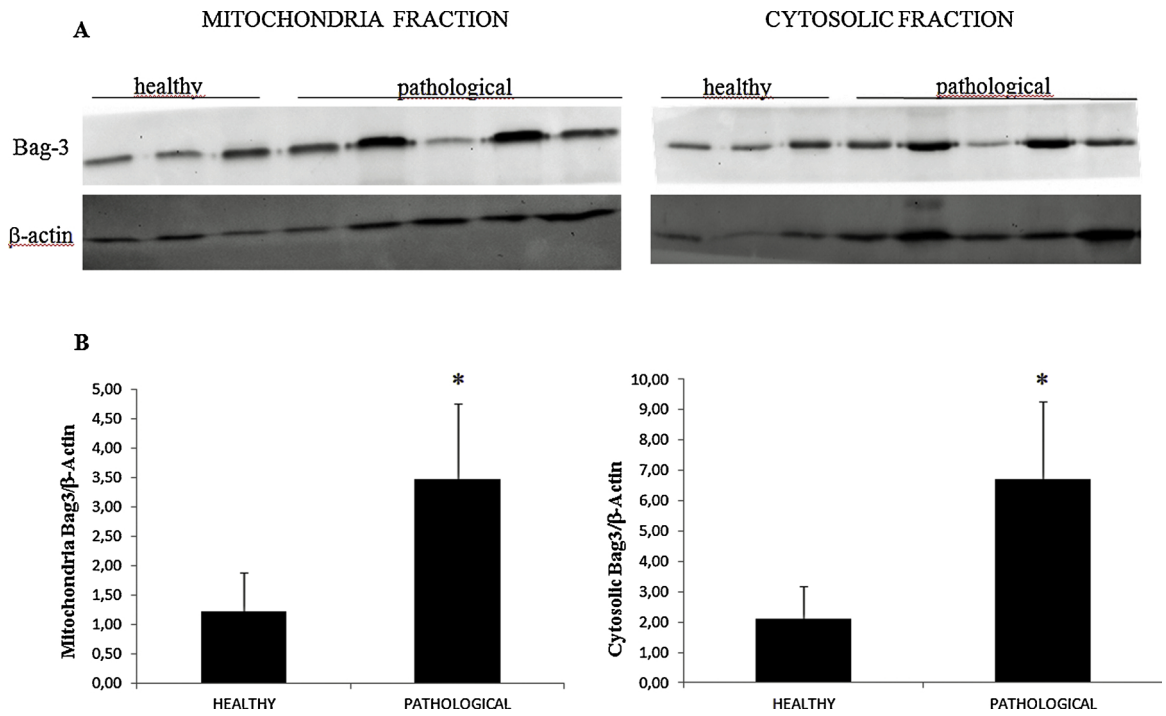

Fig. 9. Western blot analysis of Bag3 in subcellular fractions of healthy and neoplastic bladder samples. Ten micrograms of different subcellular protein fraction were hybridised with anti-Bag-3 or anti-β-actin antibody as a loading control. Densitometric analysis for mitochondrial and cytosolic Bag3 protein was performed in comparison with β-actin protein levels. The calculations were based on three independent determinations. The values for the latter are expressed as a percentage of the average values for the healthy samples (*$p < 0.05$).

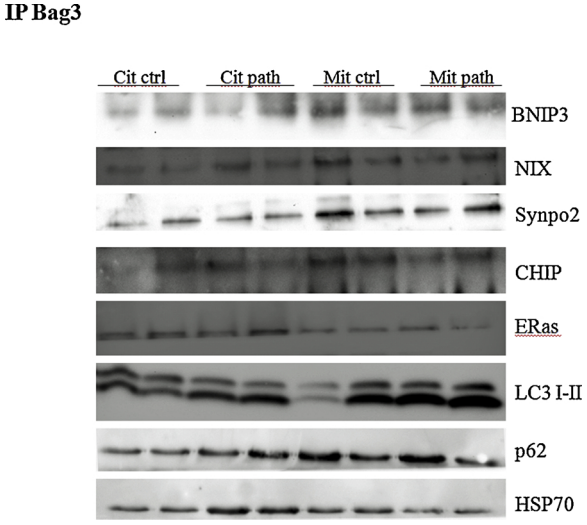

Fig. 10. Mitochondrial and cytosolic immunoprecipitation by an anti-Bag3 antibody in non-neoplastic and neoplastic bladder samples. Western blot analysis revealed the presence of BNIP3, BNIP3L/Nix, LC3, ERAS, HSP70, CHIP, p62, and Synpo2 proteins in Bag3 immunoprecipitates.

LC3, thus allowing for the engulfment of mitochondria and/or unwanted proteins by autophagosomes. Accordingly, ERAS may play an important role in mitophagosome formation. It has very recently been shown that other small GPTases, such as Rheb and Rab proteins, belonging to the Ras superfamily, play a central role in mitophagosome formation and in Parkin-dependent mitochondrial clearance (Hammerling et al., 2017). In this context, the small GTPases of the Ras gene family are known to play a crucial role in autophagy pathway (Schmukler et al., 2014).

Furthermore, we detected that BAG3 translocated to mitochondria where it interacted with both BNIP3 and BNIP3L/Nix. At the mitochondrial level, a complex composed of BNIP3/BNIP3L/Nix- Bag3-Hsc70/Hsp70 – CHIP-Synpo2/LC3/p62/ERAS was also found, suggesting that Bag3 may play a role in selective autophagy of mitochondria through mitophagy receptors. It is known that Bag3 induces selective autophagy by interacting with the autophagy receptor protein, p62, which is known to be able to interact simultaneously with the chaperone-bound cargo ubiquitylated by CHIP as well as the autophagosome membrane-associated protein LC3 (Kathage et al., 2017). Furthermore, the interaction of Bag3 with Synpo2, known to promote autophagosome formation, may contribute to further mitophagosome biogenesis. Bag3 has been shown to play a crucial role in Parkin-dependent mitophagy (Tahrir et al., 2017). Furthermore, we have previously shown that Bag3 is also involved in Parkin-independent mitophagy mediated by FUNDC1 (Roperto et al., 2019a). This study provides new mechanistic insights into the role of Bag3 in the downstream pathway of both BNIP3 and BNIP3L/Nix-mediated mitophagy. Therefore, it is conceivable that the mitochondrial complex mediated by Bag3, which is composed of mitophagy effectors, may govern the crosstalk between the distinct pathways of the Parkin-dependent and Parkin-independent mitophagy receptors as a crosstalk between mitophagy receptors and the PINK1/Parkin pathway has been suggested. These findings indicated that a redundancy may exist in the downstream degradation pathways to ensure efficient mitochondrial clearance.

To our knowledge, no studies describe mitophagy mediated by BNIP3 and BNIP3L/Nix associated with viral diseases and cancer in veterinary medicine, whereas a very limited number of studies exists in human medicine. Therefore, the potential roles of mitophagy receptors during virus carcinogenesis remain largely unknown. Several studies have suggested that viruses trigger mitophagy to promote viral replication. It has been shown that high-risk HPVs recognize several pathways to induce mitophagy, including receptor-mediated mitophagy (Hou et al., 2017; Thomas et al., 2017). Furthermore, very recently it has been shown that HPVs elicit an innate immune response via mitochondrial antiviral signalling (MAVS) (Chiang et al., 2018), thus

showing that mitochondria play an important role in immune response against PV infection.

It is conceivable that the BPV E5 oncoprotein could play a role in the BNIP3- and BNIP3L/Nix-mediated mitophagy of naturally occurring bladder cancer in cattle. The BPV E5 oncoprotein interacted with ERAS, which, in turn, was found at mitochondrial levels in a complex composed of E5/BNIP3/BNIP3L/LC3/p62. Furthermore, activation of mitophagy mediated by FUNDC1, a mitophagy receptor induced by hypoxia, has just been reported in urothelial cells infected by BPVs (Roperto et al., 2019a). Therefore, the BPV E5 oncoprotein appeared to upregulate mitophagy mediated by mitophagy receptors as reported in the following scheme:

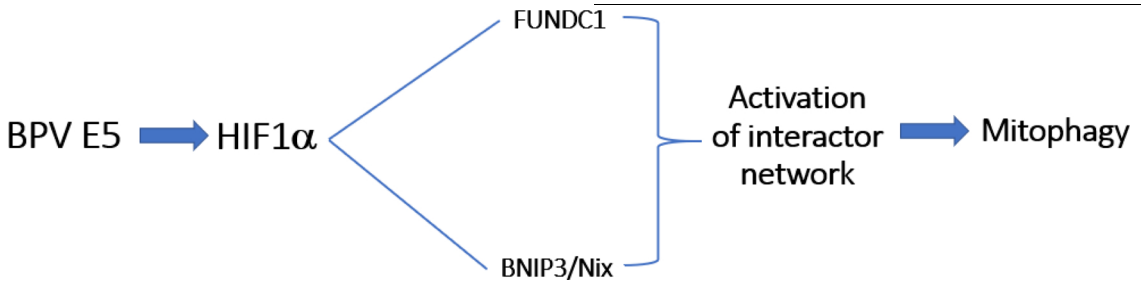

In addition, we showed that E5 oncoprotein of BPVs was responsible for the activation of a specific form of general autophagy called chaperone-assisted selective autophagy (CASA) mediated by Bag3 (Roperto et al., 2018). The BPV E5 oncoprotein is also shown to interact with a network of proteins mediated by Bag3 via its retrograde transport along microtubules to aggresome (Roperto et al., 2019b). Therefore, it is conceivable that the BPV E5 oncoprotein is a central player in autophagic flux which appears to be activated in BPV infection. It is noteworthy that autophagy is strongly impaired by being knocked down and/or inhibited in malignancy mediated by HPV infection. In this context, our findings regarding the autophagy machinery observed in BPV infection are very different from those observed in HPV infection.

It is challenging draw conclusions about the role of mitophagy in persistent infection and ultimately tumorigenesis by BPVs. However, it is conceivable that activation of mitophagy may be involved in modulating the biological behaviour of BPV-associated urothelial cancers of cattle characterised by a relatively low percentage of metastasis (8–10%) prevalent in regional lymph nodes rather than distant organs (Pamukcu, 1974; Roperto et al., 2010).

5. Conclusion

Emerging evidence supports the idea that the BPV E5 oncoprotein is a central hub of a network of protein interactors responsible for the activation of selective autophagy in urothelial cells infected by BPVs. In particular, the BPV E5 oncoprotein appears to be involved in the activation of different mitophagy modalities. However, many autophagic pathways are still unknown. Further research is needed to elucidate the detailed molecular mechanisms by which mitophagy imparts immunity against papillomavirus infections and pathogenesis. A better understanding of the mechanisms involved in oncogenesis of BPVs, which may serve as a spontaneous model of disease, can help to develop future treatment and regulatory measures for BPVs responsible for severe economic losses in cattle industry.

Funding

This research was partially supported by Regione Campania and Regione Basilicata. The funders of the work did not influence study design, data collection and analysis, decision to publish, or preparation of the manuscript.

The author(s) declare no potential conflicts of interests with respect to the research, authorship, and/or publication of this article.

Declaration of Competing Interest

The author(s) declare no potential conflicts of interests with respect to the research, authorship, and/or publication of this article.

Acknowledgements

We would like to thank Prof. D. DiMaio, Yale University, New Haven, for kindly providing an anti-E5 rabbit polyclonal antiserum; and Dr S. Morace, University of Catanzaro “Magna Graecia”; Dr G. Salvatore, Regione Basilicata; and Dr P. Sarnelli, Regione Campania for their technical help.

References

Bernardini, J.P., Lazarou, M., Dewson, G., 2017. Parkin and mitophagy in cancer. Oncogene 36, 1315–1327.
Bhujabal, Z., Birgisdottir, A.B., Sjøttem, E., Brenne, H.B., Øvervatn, A., Habisov, S., Kirkin, V., Lamark, T., Johansen, T., 2017. FKBP8 recruits LC3A to mediate Parkin-independent mitophagy. EMBO Rep. 18, 947–961.
Campo, M.S., Jarrett, W.F.H., Barron, R.J., O'Neilm, B.W., Smith, K.T., 1992. Association of bovine papillomavirus type 2 and bracken fern with bladder cancer in cattle. Cancer Res. 52, 6898–6904.
Chiang, C., Pauli, E.K., Biryukov, J., Feister, K.F., Meng, M., White, E.A., Münger, K., Howley, P.M., Meyers, C., Gack, M.U., 2018. The human papillomavirus E6 oncoprotein targets USP15 and TRIM25 to suppress RIG-I-mediated innate immune signalling. J. Virol. 92, e01737–17.
Chourasia, A.H., Boland, M.L., Macleod, K.F., 2015. Mitophagy and cancer. Cancer Metab. 3, 4. https://doi.org/10.1186/s40170-015-0130-8.
Chourasia, A.H., Macleod, K.F., 2015. Tumor suppressor functions of BNIP3 and mitophagy. Autophagy 11, 1937–1938.
Crespo, S.E.I., Lunardi, M., Otonel, R.A.A., Headley, S.A., Alfieri, A.F., Alfieri, A.A., 2019. Genetic characterization of a putative new type of bovine papillomavirus in the Xipapillomavirus 1 species in a Brazilian dairy herd. Virus Genes. https://doi.org/10.1007/s11262-019-01694-8.
Daskalaki, I., Gkikas, I., Tavernarakis, N., 2018. Hypoxia and selective autophagy in cancer development and therapy. Front. Cell Dev. Biol. 6, 104. https://doi.org/10.3389/fcell.2018.00104.
Daudt, C., Da Silva, F.R.C., Lunardi, M., Alves, C.B.D.T., Weber, M.N., Cibulski, S.P., Alfieri, A.F., Alfieri, A.A., Canal, C.W., 2018. Papillomavirus in ruminants: an update. Transbound. Emerg. Dis. 65, 1381–1395.
DiMaio, D., Petti, L., 2013. The E5 proteins. Virology 445, 99–114.
Guo, Y., Meng, X., Ma, J., Zheng, Y., Wang, Q., Wang, Y., Shang, H., 2014. Human papillomavirus 16 E6 contributes HIF-1α induced Warburg effect by attenuating the VHL- HIF-1α interaction. Int. J. Mol. Sci. 15, 7974–7986.
Hammerling, B.C., Najor, R.H., Cortez, M.Q., Shires, S.E., Leon, L.J., Gonzales, E.R., Boassa, D., Phan, S., Thor, A., Jimenez, R.E., Li, H., Kitsis, R.N., Dor, G.W.I.I., Sadoshima, J., Ellisman, M.H., Gustafsson, A.B., 2017. A Rab5 endosomal pathway mediates Parkin-dependent mitochondrial clearance. Nat. Comm. 8, 14050. https://doi.org/10.1038/ncomms14050.
Hou, H., Er, P., Cheng, J., Chen, X., Ding, X., Wang, Y., Chen, X., Yuan, Z., Pang, Q., Wang, P., Qian, D., 2017. High expression of FUNDC1 predicts poor prognostic outcomes and is a promising target to improve chemoradiotherapy effects in patients with cervical cancer. Cancer Med. 6, 1871–1881.

Kathage, B., Gehlert, S., Ulbricht, A., Lüdecke, L., Tapia, V.E., Orfanos, Z., Wenzel, D., Bloch, W., Volkmer, R., Fleishmann, B.K., Fürst, D.O., Höhfeld, J., 2017. The co-chaperone BAG3 coordinates protein synthesis and autophagy under mechanical strain through spatial regulation of mTORC1. Biochim. Biophys. Acta 1864, 62–75.

Lampert, L.A., Orogo, A.M., Najor, R.H., Hammerling, B.C., Leon, L.J., Kim, T., Sussman, M.A., Gustafsson, A.B., 2019. BNIP3L/NIX and FUNDC1-mediated mitophagy is required for mitochondrial network remodeling during cardiac progenitor cell differentiation. Autophagy 11, 1–17.

Liu, L., Sakakibara, K., Chen, Q., Okamoto, K., 2014. Receptor-mediated mitophagy in yeast and mammalian systems. Cell Res. 24, 787–795.

Mattoscio, D., Medda, A., Chiocca, S., 2018. Human papilloma virus and autophagy. Int. J. Mol. Sci. 19, 1775. https://doi.org/10.3390/ijms19061775.

Melser, S., Chatelain, E.H., Lavie, J., Mahfouf, W., Jose, C., Obre, E., Goorden, S., Priault, M., Elgersma, Y., Rezvani, H.R., Rossignol, R., Bénard, G., 2013. Rheb regulates mitophagy induced by mitochondrial energetic status. Cell Metab. 17, 719–739.

Moyzis, A., Gustafsson, A.B., 2019. Multiple recycling routes: canonical vs non-canonical mitophagy in the heart. Biochim. Biophys. Acta – Mol. Basis Dis. 1865, 797–809.

Nakamura, M., Bodily, J.M., Berglin, M., Kyo, S., Inoue, M., Laimins, L.A., 2009. Hypoxia-specific stabilization of HIF-1alfa by human papillomaviruses. Virology 387, 442–448.

Ney, P.A., 2015. Mitochondrial autophagy: origins, significance, and role of BNIP3 and NIX. Biochim. Biophys. Acta 1853, 2775–2783.

Pamukcu, A.M., 1974. Tumours of the urinary bladder. Bull. Wld. Hlth. Org. 50, 43–52.

Pickles, S., Vigié, P., Youle, R.J., 2018. Mitophagy and quality control mechanisms in mitochondrial maintenance. Curr. Biol. 28, R170–R185.

Rodolico, V., Arancio, W., Amato, M.C., Aragona, F., Cappello, F., di Fede, O., Pannone, G., Campisi, G., 2011. Hypoxia inducible factor-1 alfa expression is increased in infected positive HPV16 DNA oral squamous cell carcinoma and positively associated with HPV16 E7 oncoprotein. Infect. Agent. Cancer 6 (18). https://doi.org/10.1186/1750-9378-6-18.

Rogov, V.V., Suzuki, H., Marinkovic, M., Lang, V., Kato, R., Kavasaki, R., Bulijubasic, M., Sprung, M., Rogova, N., Wakatsuki, S., Hamacher-Brady, A., Dötsch, V., Dikic, I., Brady, N.R., Novak, I., 2017. Phosphorylation of the mitochondrial autophagy receptor Nix enhances its interaction with LC3 proteins. Sci. Rep. 7, 1131. https://doi.org/10.1038/s41598-017-01258-6.

Roperto, S., Borzacchiello, G., Brun, R., Leonardi, L., Maiolino, P., Martano, M., Paciello, O., Papparella, S., Restucci, B., Russo, V., Salvatore, G., Urraro, C., Roperto, F., 2010. A review of bovine urothelial tumours and tumour-like lesions of the urinary bladder. J. Comp. Pathol. 142, 95–108.

Roperto, S., Russo, V., De Falco, F., Rosati, A., Catoi, C., Roperto, F., 2019a. FUNDC1-mediated mitophagy in bovine papillomavirus-infected urothelial cells. Vet. Microbiol. https://doi.org/10.1016/j.vetmic.2019.05.017.

Roperto, S., Russo, V., De Falco, F., Urraro, C., Maiolino, P., Del Piero, F., Roperto, F., 2019b. Bovine papillomavirus E5 oncoprotein expression and its association with an interactor network in aggresome-autophagy pathway. Vet. Microbiol. 233, 39–46.

Roperto, S., Russo, V., Leonardi, L., Martano, M., Corrado, F., Riccardi, M.G., Roperto, F., 2016. Bovine papillomavirus type 13 expression in the urothelial bladder tumours of cattle. Transbound. Emerg. Dis. 63, 628–634.

Roperto, S., Russo, V., Ozkul, A., Sepici-Dincel, A., Maiolino, P., Borzacchiello, G., Marcus, I., Esposito, I., Riccardi, M.G., Roperto, F., 2013. Bovine papillomavirus type 2 infects the urinary bladder of water buffalo (Bubalus bubalis) and plays a crucial role in bubaline urothelial cancerogenesis. J. Gen. Virol. 94, 403–408.

Roperto, S., Russo, V., Rosati, A., Ceccarelli, D.M., Munday, J.S., Turco, M.C., Roperto, F., 2018. Chaperone-assisted selective autophagy in healthy and papillomavirus-associated neoplastic urothelium of cattle. Vet. Microbiol. 221, 134–142.

Roperto, S., Russo, V., Urraro, C., Restucci, B., Corrado, F., De Falco, F., Roperto, F., 2017. ERas is constitutively expressed in full term placenta of pregnant cows. Theriogenology 193, 162–168.

Russo, V., Roperto, F., Esposito, I., Ceccarelli, D.M., Zizzo, N., Leonardi, L., Capparelli, R., Borzacchiello, G., Roperto, F., 2016. ERas protein is overexpressed and binds to the activated platelet-derived growth factor β receptor in bovine urothelial cells associated with papillomavirus infection. Vet. J. 212, 44–47.

Russo, V., Roperto, F., Taulescu, M., De Falco, F., Urraro, C., Corrado, F., Munday, J.S., Catoi, C., Roperto, S., 2019. Expression of the feline leukemia virus subgroup C receptors in normal and neoplastic urothelium of the urinary bladder of cattle associated with bovine papillomavirus infection. Vet. Microbiol. 229, 147–152.

Schlegel, R., Wade-Glass, M., Rabson, M.S., Yang, Y.C., 1986. The E5 transforming gene of bovine papillomavirus encodes a small hydrophobic protein. Science 233, 464–467.

Schmukler, E., Kloog, Y., Pinkas-Kramarski, 2014. Ras and autophagy in cancer development and therapy. Oncotarget 5, 576–586.

Springer, M.Z., Macleod, K.F., 2016. Mitophagy: mechanisms and role in human disease. J. Pathol. 240, 253–255.

Tahrir, F.G., Knezevic, T., Gupta, M.K., Gordon, J., Cheung, J.Y., Feldman, A.M., Khalili, K., 2017. Evidence for the role of Bag3 in mitochondrial quality control in cardiomyocytes. J. Cell. Physiol. 232, 797–805.

Takahashi, K., Nakagawa, M., Young, S.G., Yamanaka, S., 2005. Differential membrane localization of Eras and Rheb, two Ras-related proteins involved in the phosphatidylinositol 3-kinase/mTOR pathway. J. Biol. Chem. 280 32768-32744.

Thomas, R.J., Oleinik, N., Selvam, S.P., Vaena, S.G., Dany, M., Nganga, R.N., Depalma, R., Baron, K.D., Kim, J., Szulc, Z.M., Ogretmen, B., 2017. HPV/E7 induces chemotherapy-mediated tumor suppression by ceramide-dependent mitophagy. EMBO Mol. Med. 9, 1030–1051.

Wei, Y., Chiang, W.C., Sumpter Jr, R., Mishra, P., Levine, B., 2017. Prohibitin 2 is an inner mitochondrial membrane mitophagy receptor. Cell 168, 224–238.

Wei, H., Liu, L., Chen, Q., 2015. Selective removal of mitochondria via mitophagy: distinct pathways for different mitochondrial stresses. Biochim. Biophys. Acta 1853, 2784–2790.

Youle, R.J., Narendra, D.P., 2011. Mechanisms of mitophagy. Nat. Rev. Mol. Cell Biol. 12, 9–14.

Zhang, L., Ney, P.A., 2009. Role of BNIP3 and NIX in cell death, autophagy, and mitophagy. Cell Death Diff. 16, 939–946.

Zhang, L., Ney, P.A., 2011. Mechanisms and biology of B-cell leukemia/lymphoma 2/Adenovirus E1B interacting protein 3 and Nip-like protein X. Antioxid. Redox Signal. 14, 1959–1969.